PERGAMON

Chemical Engineering Science 54 (1999) 2527–2533

Chemical Engineering Science

Modeling of heat transfer in wall-cooled tubular reactors

G.W. Koning*, K.R. Westerterp

Department of Chemical Technology, University of Twente, P.O. Box 217, 7500 AE Enschede, Netherlands

Abstract

In a pilot scale wall-cooled tubular reactor, temperature profiles have been measured with and without reaction. As a model reaction oxidation of carbon monoxide in air over a copper chromite catalyst has been used. The kinetics of this reaction have been determined separately in two kinetic reactors with internal recycle. A pseudo-homogeneous reactor model without axial dispersion is used for the description of the temperature profiles inside the reactor. The heat transport parameters $\lambda_{rad,eff}$ and α_w have been optimized to give optimum agreement between experimental and calculated temperature profiles. Preliminary experiments showed that the occurrence of reaction seems to increase the overall heat transfer coefficient. The pseudo-homogeneous reactor model is allowed to be used, but is not adequate for the description of the temperature profiles inside the reactor during reaction.

Keywords: Heat transfer; Tubular packed carbon monoxide

1. Introduction

For a proper design of a wall-cooled tubular reactor an accurate knowledge of the heat transfer properties of the catalyst bed is required because of the high parametric sensitivity of the reactor behavior towards parameters such as inlet- and wall temperature, gas velocity, pressure and inlet concentration. When operating the reactor, it is desirable to operate as close as possible to runaway conditions because this will give maximum capacity.

Nowadays most cooled tubular reactors are not designed on the basis of kinetic data and model calculations, but experiments are carried out using single tubes in pilot scale reactors at practical conditions. Previous studies of heat transport phenomena in wall-cooled tubular reactors have shown a discrepancy between the effective radial conductivities of the catalyst bed measured with and without reaction (Hall et al. 1949; Hoffman et al. 1979; Schwedock et al. 1989; Schouten et al. 1994). Schwedock et al., 1989) found that the radial heat conductivity was about 50% higher in the presence of reaction than when no reaction occurs. Borman and Schouten (Schouten et al., 1994) used partial oxidation of ethylene to ethylene oxide over a silver/γ-alumina catalyst in their work. The main disadvantages of this reaction system is its complicated kinetics, caused by the occurrence of complete combustion of ethylene as a parallel reaction, the large number of reactants that influence the reaction rate and a slow deactivation of the catalyst. This investigation is a continuation of their work using more simple kinetics. The oxidation of carbon monoxide to carbon dioxide over a copper chromite catalyst has been chosen as model reaction. An advantage of this reaction is its large enthalpy of reaction of 283 kJ mol^{-1}, which causes a large temperature increase at a small change in the composition of the gas mixture. Two different reactors with internal recycle were used for the determination of the reaction rate.

2. Heat transfer measurements

Heat transfer experiments have been carried out in a pilot scale wall-cooled tubular reactor with a length of 1 m and a diameter of 53.1 mm (Fig. 1).

The compressed air feed is purified in oil-filters, a two-column regenerative adsorption dryer and an active carbon filter. A buffer vessel is used to damp pressure fluctuations. The air and carbon monoxide (99.9%

* Corresponding author. Tel.: 0031 53 489 3047; fax: 0031 53 489 4738; e-mail: g.w.koning@ct.utwente.nl

0009-2509/99/$ – see front matter
PII: S0009-2509(98)00471-0

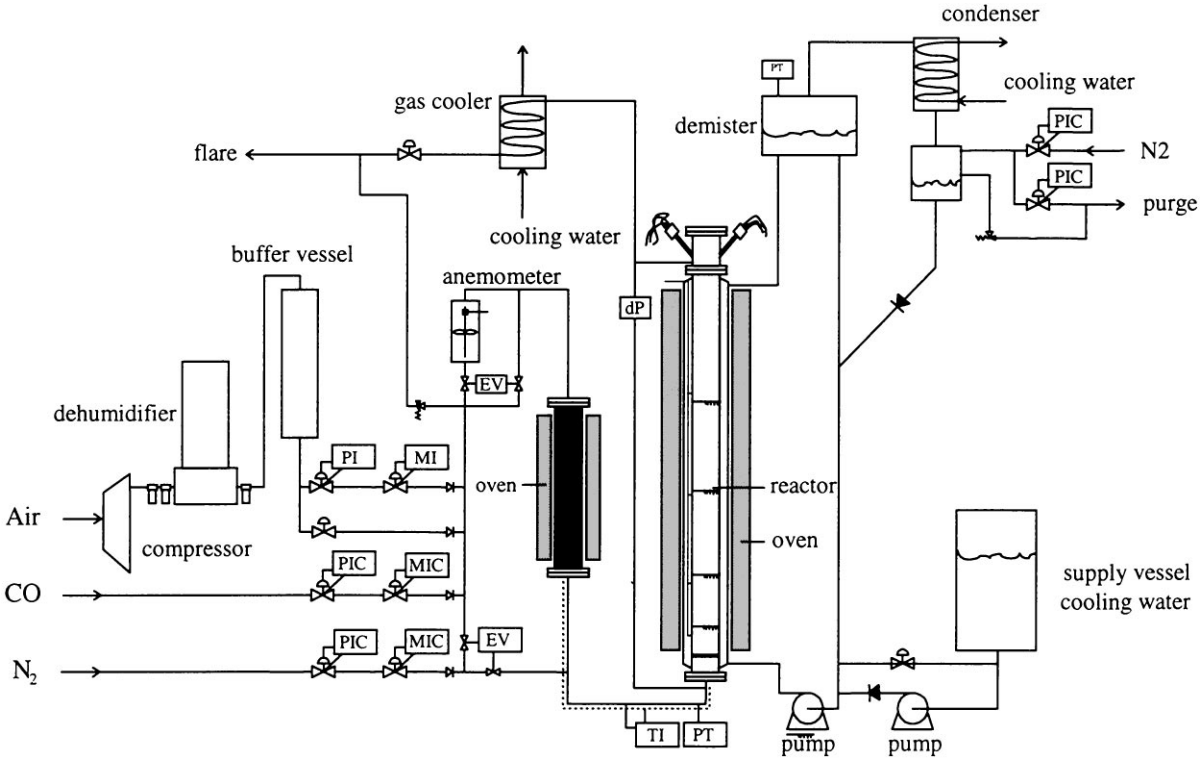

Fig. 1. Experimental setup of the cooled tubular reactor.

purity) flow rate are controlled with electronic mass flow controllers. The maximum gas flux in the reactor is 6.8 kg m^{-2} s^{-1} at pressures of 3–9 bar. The combined flow rate of the gas mixture is measured with a propeller anemometer. The gas mixture is preheated in an electrically heated tube filled with steel particles. A tracing coiled around the feed tube is used to control the temperature of the gas fed to the reactor. The pressure in the gas system is measured in the buffering vessel and at the reactor inlet with electronic pressure transmitters. A differential pressure transmitter connected to the inlet and outlet of the reactor measures the pressure drop over the catalyst bed.

The reactor wall is cooled by pressurized boiling water that is pumped through the cooling jacket surrounding the reactor. The wall temperature can be controlled by varying the pressure in the cooling water loop from 1 to 40 bar. The wall temperature is measured at 4 axial positions using type K thermocouples with a diameter of 0.5 mm. The maximum temperature difference along the wall is less then 1°C at the most extreme conditions near runaway operation. In experiments without reaction the cooling water is kept at its boiling point by an electrically heated oven surrounding the cooling jacket. The cylindrical catalyst pellets have a height of 5.03 mm and a diameter of 4.85 mm; the bed porosity is 0.357. Inside the reactor 36 type K themocouples with a diameter of 0.5 mm are fixed in a thermocouple ladder. This ladder consists of two metal wires in between which beams made of poly-ether-ether-keton (PEEK) with a heat conductivity 0.4 W m^{-1} K^{-1} are placed to hold the thermocouples. The gas temperature profile is measured at distances of 0, 8, 16, 21 and 25 mm from the center line of the tube at 6 axial positions. At each axial position also the temperature of a catalyst particle at 8 mm from the tube center line is measured by inserting a thermocouple inside a particle. The first radial profile is measured just after the gas distributor plate.

At 8 axial positions a sample of the gas mixture can be withdrawn from the reactor at the wall. The carbon dioxide concentration is analyzed with an infrared gas analyzer.

A Hewlett Packard Data Acquisition and Control Unit connected to a PC is used for data collection and process control. The entire experimental setup has been installed in a concrete bunker and is controlled from the outside. The reactor can be automatically shut down and purged with nitrogen in case of an emergency like exceeding of a preset maximum temperature or carbon monoxide concentration, a power failure or a crash of controlling software.

Fig. 2 shows a measured temperature profile without reaction. Fig. 5 shows a temperature profile measured with reaction at conditions close to runaway. In the first graph it can be seen that the radial inlet temperature profile is almost completely flat in the middle of the bed.

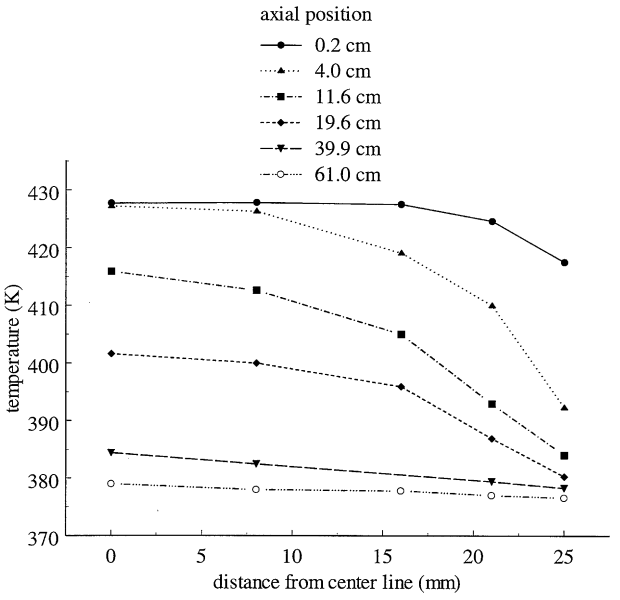

Fig. 2. Example of measured radial temperature profiles without reaction.

The influence of the wall can only be observed at 1 mm from the wall.

3. Reactor modeling

The temperature and concentration profiles measured are described with a heterogeneous model in which heat- and mass transfer is described according to the Fourier law for heat dispersion and Fick law for mass dispersion:

$$\lambda_{\mathrm{rad,eff}}\frac{1}{r}\frac{\partial}{\partial r}\left(r\frac{\partial T_g}{\partial r}\right)-u_s\rho_g c_{p,g}\frac{\partial T_g}{\partial z}+\alpha_p(T_s-T_g)=0, \tag{1}$$

$$\rho_s(1-\varepsilon)R(C_{\mathrm{CO},s},T_s)\Delta H_R-\alpha_p(T_s-T_g)=0,$$

$$D_{\mathrm{rad,eff}}\frac{1}{r}\frac{\partial}{\partial r}\left(r\frac{\partial C_{\mathrm{CO},g}}{\partial r}\right)-u_s\frac{\partial C_{\mathrm{CO},g}}{\partial z}+k_g(C_{\mathrm{CO},s}-C_{\mathrm{CO},g})=0, \tag{2}$$

$$\rho_s(1-\varepsilon)R(C_{\mathrm{CO},s},T_s)-k_g(C_{\mathrm{CO},s}-C_{\mathrm{CO},g})=0,$$

using the following boundary conditions:

$$r=0\quad \frac{\partial T_g}{\partial r}=0,\qquad \frac{\partial C_{\mathrm{CO},g}}{\partial r}=0,$$

$$r=R\quad -\lambda_{\mathrm{rad,eff}}\frac{\partial T_g}{\partial r}-\alpha_w(T_g-T_w)=0,\quad \frac{\partial C_{\mathrm{CO},g}}{\partial r}=0. \tag{3}$$

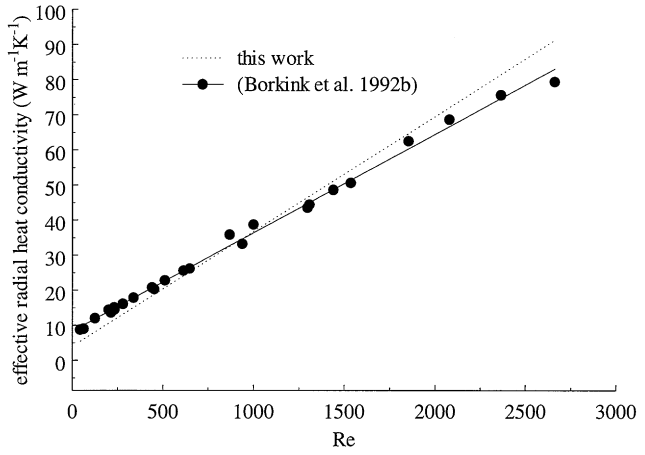

Fig. 3. Effective radial heat conductivity $\lambda_{\mathrm{rad,eff}}$ as a function of the Reynolds number, compared to the values reported by (Borkink et al., 1992b).

In case of small differences in concentration and temperature between the gas phase and the solid phase the reactor contents can be regarded as a continuum in the modeling of radial heat and mass transfer. In that case a pseudo-homogeneous model can be used.

It has been assumed that the radial velocity profile is flat and that axial dispersion can be neglected (Borkink et al., 1992a). The radial dispersion of heat has been assumed to be located in the gas phase only. Temperature and concentration profiles were numerically calculated solving the partial differential equations according to the method of finite differences using Crout's algorithm. The heat transfer parameters α_w and $\lambda_{\mathrm{rad,eff}}$ were optimized to give a minimum relative difference between the measured and the calculated dimensionless gas temperature $\Theta=(T_g-T_{\mathrm{inlet}})/\Delta T_{\mathrm{ad}}$ in case of reaction or $\Theta=(T_g-T_{\mathrm{inlet}})/(T_w-T_{\mathrm{inlet}})$ in case of no reaction.

In Figs. 3 and 4 $\lambda_{\mathrm{rad,eff}}/\lambda_g$ and the Nusselt number $\alpha_w d_{p,\mathrm{eff}}/\lambda_g$ are plotted as a function of the Reynolds number for experiments without reaction. In the experiments used for this plot the average gas temperature is about 400 K.

The superficial gas velocity has been varied from 0.1 to 0.5 m s^{-1} at pressures from 2 to 8 bar. The effective radial conductivity can be described within 5% error with:

$$\lambda_{\mathrm{rad,eff}}/\lambda_g=8.3+0.028Re. \tag{4}$$

Re in this equation is based on the interstitial gas velocity and an effective particle diameter as calculated with

$$d_{p,\mathrm{eff}}=6V_p/A_p. \tag{5}$$

Because of the strong cross-correlation between $\lambda_{\mathrm{rad,eff}}$ and α_w the fitted values of the wall heat transfer coefficient show a rather large scatter compared to the

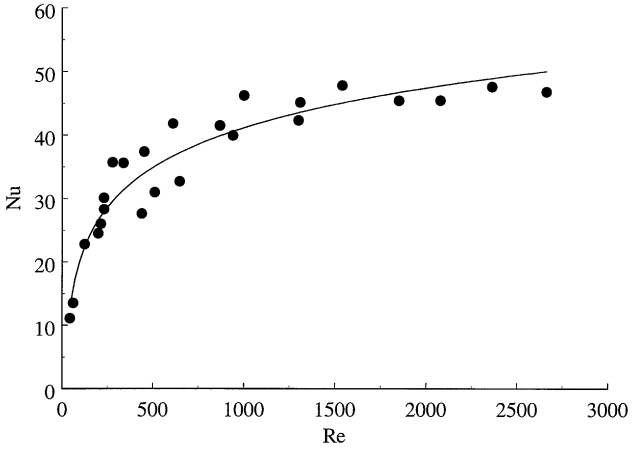

Fig. 4. Nusselt number as a function of the Reynolds number.

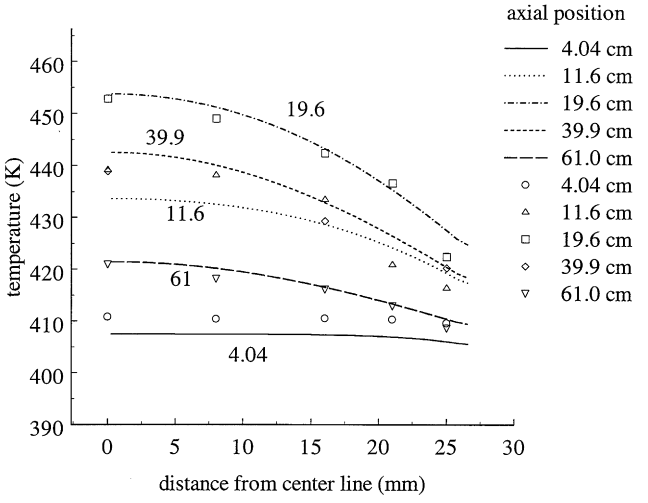

Fig. 5. Calculated (lines) and measured (dots) radial temperature profiles ($P = 5.15$ bar, $v_s = 0.58\ \mathrm{m\,s^{-1}}$, $c_{\mathrm{CO,inlet}} = 1.37\ \mathrm{mol\,m^{-3}}$, $T_{\mathrm{wall}} = 401$ K, $\lambda_{\mathrm{rad,eff}} = 2.65$, $\alpha_w = 251$).

scatter in the values of $\lambda_{\mathrm{rad,eff}}$, caused by the insensitivity of the model results towards α_w at high values of the Biot number. For this reason, the values of α_w have been fitted to the experimental data a second time, using Eq. (4). For the calculation of the Nusselt number as a function of the Reynolds number the following equation has been obtained:

$$Nu = \alpha_w d_{p,\mathrm{eff}}/\lambda_g = 6.97 Re^{0.25}. \tag{6}$$

Experiments with reaction have been carried out in the same catalyst bed without repacking at the following operating conditions: $4 < P < 7$ bar, $900 < Re < 1650$, $119 < T_w < 129^{\circ}\mathrm{C}$, $112 < T_{\mathrm{inlet}} < 139^{\circ}\mathrm{C}$ and $0.5 < c_{\mathrm{CO,inlet}} < 2\ \mathrm{mol\ m^{-3}}$.

Again the heat transport parameters $\lambda_{\mathrm{rad,eff}}$ and α_w in the reactor model are optimized to obtain a minimum relative difference between the measured and the calculated dimensionless temperature profile, whereas reaction kinetics used in the model had been obtained from kinetic experiments in two different kinetic reactors with internal recycle (see further). From model simulations it was found that the radial variation of the concentrations can be neglected. Using correlations for the heat and mass transfer between particles and fluids in packed beds that have been derived by Gnielinski (1982), the maximum error in $\lambda_{\mathrm{rad,eff}}$ and α_w caused by neglect of heat- and mass-transfer resistance between the solid phase and the gas phase was found to be approximately 3% at the most extreme conditions. Westerterp (Wijngaarden et al., 1989) derived a criterion as to whether or not a homogeneous model can be used instead of a heterogeneous model in describing wall-cooled tubular reactors, introducing a dimensionless parameter ς:

$$\zeta = \frac{|\Delta H_R| V_p}{(1-\varepsilon)\alpha_p A_p} \frac{\partial R(T)}{\partial T}\bigg|_{T=T_w} = \frac{R(T_g) - R(T_g)}{R(T_s)}. \tag{7}$$

ς is a measure for the relative increase in reaction rate due to the external heat transfer resistance between the catalyst pellet and the gas. If a maximum error of 10% is allowed in the parameters $\lambda_{\mathrm{rad,eff}}$, α_w, ς should have a value less than or equal to 0.1. For the experiments used the maximum value of ς did not exceed a value of 0.03. As a consequence, we can further use a pseudo-homogeneous reactor model.

Fig. 5 shows a measured temperature profile and the corresponding calculated one. In Fig. 6 the calculated axial concentration profile is compared to the measured profile. The values of the parameters $\lambda_{\mathrm{rad,eff}}$ and α_w for experiments with and without reaction are different from those obtained from experiments without reaction. The values of $\lambda_{\mathrm{rad,eff}}$ as obtained from experiments with reaction have increased by a factor 1.6 to 1.8 compared to those as obtained from experiments without reaction, whilst the values of α_w have decreased by a factor 1.1 to 1.5.

Dixon (1996) proposed the following equation for the calculation of the overall heat transfer coefficient U from $\lambda_{\mathrm{rad,eff}}$ and α_w:

$$\frac{1}{U} = \frac{1}{\alpha_w} + \frac{R_t}{3\lambda_{\mathrm{rad,eff}}} \frac{Bi+3}{Bi+4} \tag{8}$$

in which R_t is the tube radius and Bi the Biot number, defined as

$$Bi = \alpha_w R_t/\lambda_{\mathrm{rad,eff}}. \tag{9}$$

In our case the ratio of the tube diameter to the particle diameter $2R_t/d_p$ is approximately 11. In Fig. 7 the overall heat transfer coefficient U is shown as a function of the Reynolds number for experiments with and without reaction. In this graph it can be seen that in case of reaction the overall heat transfer coefficient increases in a similar manner as in the case in which there is no reaction. For

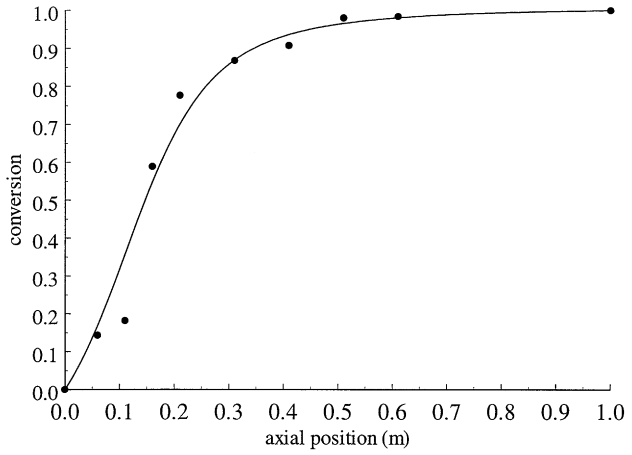

Fig. 6. Calculated (line) and measured (dots) carbon monoxide conversion ($P = 5.15$ bar, $v_s = 0.58\ m\,s^{-1}$, $c_{CO,inlet} = 1.37\ mol\,m^{-3}$, $\lambda_{rad,eff} = 2.65$, $\alpha_w = 251$).

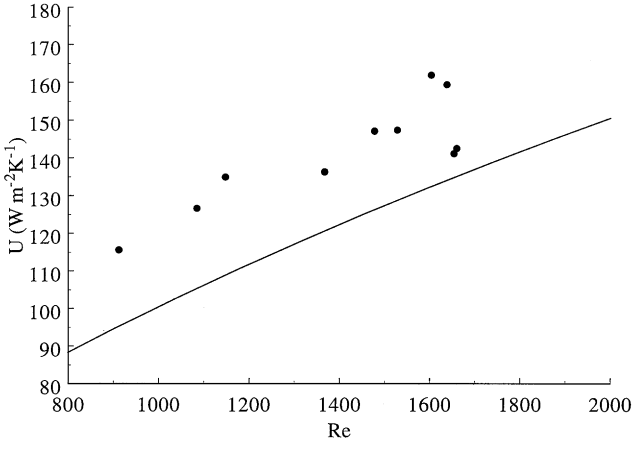

Fig. 7. Comparison of the overall heat transfer coefficient without (line) and with (dots) reaction ($4 < P < 7$ bar, $900 < Re < 1650$, $119 < T_{wall} < 129°C$, $112 < T_{inlet} < 139°C$ and $0.5 < c_{CO,inlet} < 2\ mol\,m^{-3}$).

all experiments with reaction the value of the overall heat transfer coefficient is a little higher than for experiments without reaction.

Further experiments will be carried out in a broader region of experimental conditions, especially at conditions at which more severe demands are made on reactor models. At high temperatures and carbon monoxide concentrations, heat- and mass-transfer resistance between the gas bulk and the catalyst and radial dispersion of mass cannot be neglected. At these conditions, especially at low ratios of tube to particle diameter, the use of Fourier's and Fick's law for the description of radial heat and mass transport becomes questionable (Westerterp et al., 1996). Comparison of temperature- and concentration profiles after repeated refilling of the reactor should give more insight in the effect of the geometrical randomness of the packing (Schouten et al., 1996).

4. Kinetic study

The kinetics of carbon monoxide oxidation have been studied in two different internal recycle reactors. The first one is a commercially available 'Berty'-type reactor (Berty, 1974). The second reactor, the so called 'BoBo'-reactor (Borman et al., 1994) has been developed in our research group. A scheme of this reactor is shown in Fig. 8.

Nitrogen of 99.99% purity, compressed air and carbon monoxide of 99.9% purity are mixed after flow rate measurement in electronic mass flow controllers; the total flow rate is maximum 3000 ml min^{-1}. The pressure inside the reactors can be varied between 1 and 10 bar and is controlled with electronic back-pressure controllers. The carbon monoxide and the carbon dioxide concentration are analyzed with an infrared gas analyzer. A PC is used for process control and data acquisition. In the Berty reactor the gas is recycled through a stationary catalyst bed by an impeller at the bottom of the reactor. In the BoBo reactor the catalyst particles are rotating with the impeller. The pressure drop over the impeller blades causes a high gas flow rate through the blades. In the Berty reactor the maximum rotational speed of the impeller is 1200 rpm, resulting in a value of the Sherwood number of 5. The rotational speed of the impeller in the BoBo reactor can be increased up to 2500 rpm., resulting in a Sherwood number of 40 for the stationary catalyst pellet and 80 for the rotating catalyst particles. The conversion should be independent towards the rotational speed of the impeller in case of ideal mixing of the reaction gas mixture and no external heat and mass transfer resistance around the catalyst pellets.

At first palladium on γ-alumina was used as a catalyst for the oxidation of carbon monoxide. This catalyst

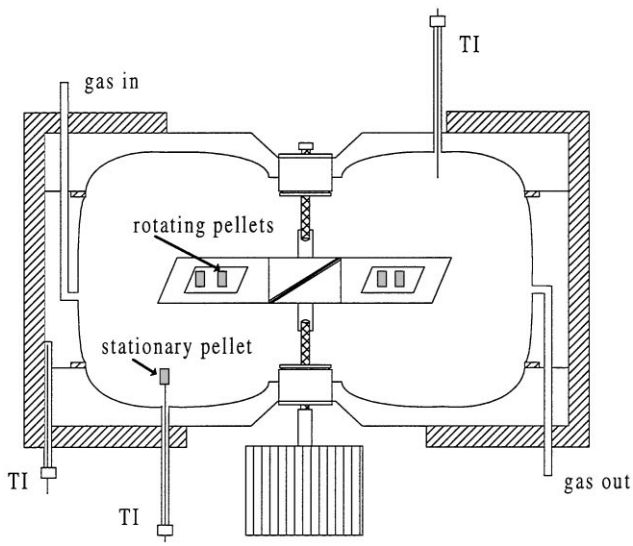

Fig. 8. Scheme of 'Bobo' reactor.

showed multiplicity of the steady state over a wide range of reaction conditions, making it impossible to derive a rate equation covering the entire region of desired reaction conditions.

Because catalyst based on transition metals are reported to not show multiplicity a copper chromite catalyst was chosen as new catalyst. The copper chromite catalyst particles of Engelhard contain 67–77 wt% copper oxide and 20–30 wt% copper chromite. This catalyst has an overall density of 2580 kg m^{-3}, a porosity of 0.4 and an average pore size of 50 nm.

Dekker et al. (1992) studied the kinetics of carbon monoxide oxidation over Cu–Cr/γ-alumina. According to this author CuO is the most active species, whilst Cr_2O_3 is mainly used to stabilize the catalyst to avoid sintering of the Cu phase. Their paper also includes am overview of kinetic investigations of the carbon monoxide oxidation over Cu-based catalysts. The reaction generally is of zeroth order in oxygen and with a positive order, smaller than one, in carbon monoxide. It is assumed that the copper is oxidized by oxygen, followed by reduction by carbon monoxide. Possible redox couples are $Cu–Cu^+$ and $Cu^+–Cu^{++}$. Mardanova measured the kinetics of carbon monoxide over Cu, Cr and Cu–Cr on γ-alumina (Mardanova et al., 1994).

It was found that, with an average difference between measured and calculated reaction rates of 14%, the reaction rate of carbon monoxide oxidation over the copper chromite catalyst can be described with the following equation:

$$R = \frac{k_r b_{CO} p_{CO}}{1 + b_{CO} p_{CO} + b_{O_2} p_{O_2}} \tag{10}$$

with

$$k_r = k_{r,0} e^{-E_{act}/RT}, \quad b_i = b_{i,0} e^{\Delta H_{ads}/RT}$$

In Fig. 9 the calculated reaction rates are plotted against the reaction rates measured in the BoBo-reactor for $350 < p_{CO} < 15\,000$ Pa, $12\,000 < p_{O_2} < 112\,000$ Pa, $90 < T < 200$°C and $0.2 < P < 0.6$ MPa. The parameters in Eq. (10) are listed in Table 1.

At catalyst temperatures up to 170°C no significant difference was found between the reaction rates measured in both reactors. At higher temperatures the reaction rate measured in the Bobo reactor becomes higher due to the occurrence of mass transfer limitation in the Berty reactor.

Eq. (10) does not have a realistic theoretical background, which can be concluded directly from the negative value of the fitted adsorption enthalpy of carbon monoxide. Further measurements have to be carried out to investigate the influence of the product carbon dioxide. For an accurate the description of the reaction rate at high temperatures the particle effectiveness should be taken into account.

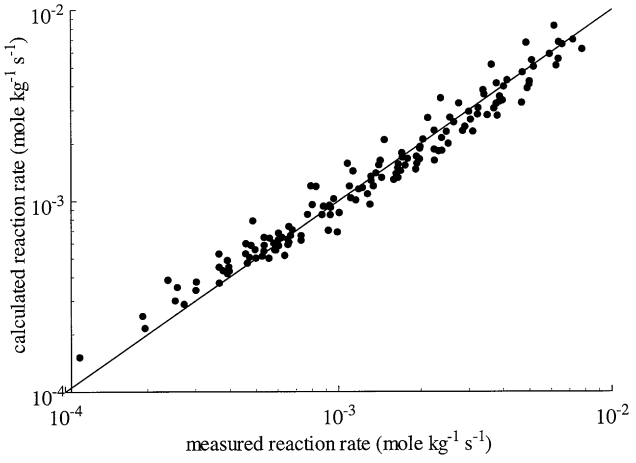

Fig. 9. Calculated versus measured reaction rates for the oxidation of carbon monoxide with air over $CuCr_2O_4$ ($0.08 < C_{CO} < 4$ mol m^{-3}, $5 < C_{O_2} < 35$ mol m^{-3}, $90 < T < 200$°C and $2 < P < 6$ bar).

Table 1
Fitting parameters reaction rate

Parameter		Value
$k_{r,0}$	(mol kg^{-1} s^{-1})	3.97×10^4
E_{act}/R	(K)	6890
$b_{CO,0}$	(Pa^{-1})	6.81×10^{-8}
$\Delta H_{ads,CO}/R$	(K)	-3680
$b_{O_2,0}$	(Pa^{-1})	3.08×10^{-5}
$\Delta H_{ads,O_2}/R$	(K)	306

5. Conclusions

In a wall-cooled tubular reactor temperature profiles have been measured in experiments with and without reaction. The kinetics of the oxidation of carbon monoxide in air over a copper chromite catalyst have been studied in two kinetic reactors with internal recycle. Optimization of the heat transfer parameters $\lambda_{rad,eff}$ and α_w in a two-dimensional heterogeneous reactor model without axial dispersion resulted in different values of these parameters for experiments with and without reaction. Combination of $\lambda_{rad,eff}$ and α_w in an overall heat transfer coefficient U shows that the overall heat transfer coefficient seems to increase due to reaction. Further experimental work is needed to obtain a more accurate description of the reaction kinetics at high reaction rates. Fig. 5 shows that the pseudo-homogeneous reactor model is inadequate for the description of the temperature profiles in a wall-cooled tubular reactor. In a following article we will explain why this is the case.

Notation

A_p	external surface particle, m^2
$b_{i,0}$	adsorption rate constant, Pa^{-1}

Bi	Biot number ($=\alpha_w R_t/\lambda_{\mathrm{rad,eff}}$)
c	concentration, mol m^{-3}
c_p	specific heat, J $kg^{-1} K^{-1}$
$d_{p,\mathrm{eff}}$	effective particle diameter, m
$D_{\mathrm{rad,eff}}$	effective radial mass dispersion coeff., mol $m^{-1} s^{-1}$
ΔH_R	reaction enthalpy, J mol^{-1}
k_g	particle mass transfer coefficient, mol $m^{-2} s^{-1}$
k_r	pre-exponential constant reaction rate, mol $kg^{-1} s^{-1}$
Nu	Nusselt number ($=\alpha_w d_{p,\mathrm{eff}}/\lambda_g$)
p	partial pressure, Pa
r	radial position, m
R	reaction rate, mol $kg^{-1} s^{-1}$
R_t	tube radius, m
Re	Reynolds number ($=\rho_g u_i d_{p,\mathrm{eff}}/\eta$)
T	temperature, K
u_i	interstitial gas velocity, m s^{-1}
u_s	superficial gas velocity, m s^{-1}
V_p	volume particle, m^3
z	axial position, m

Greek letters

α_p	particle heat transfer coefficient, W $m^{-2} K^{-1}$
α_w	wall heat transfer coefficient, W $m^{-2} K^{-2}$
ε	bed porosity, dimensionless
η	dynamic viscosity, Pa s
θ	dimensionless temperature ($=(T-T_w)/(T_{\mathrm{inlet}}-T_w)$ or $(T-T_{\mathrm{inlet}})/(\Delta T_{\mathrm{ad}})$)
λ	heat conductivity, W $m^{-1} K^{-1}$
$\lambda_{\mathrm{rad,eff}}$	effective radial heat conductivity, W $m^{-1} K^{-1}$
ρ	density, kg m^{-3}

Subscripts

c	catalyst
calc	calculated value
eff	effective
g	gas phase
meas	measured value
rad	radial
s	solid phase
w	wall

References

Berty, J.M. (1974). Reactor for vapor-phase catalytic studies, *Chem. Engng Prog.*, *70*, 78–84.

Borkink, J.G.H., & Westerterp, K.R. (1992). Significance of axial heat dispersion for the description of heat transport in wall-cooled packed beds. *Chem. Engng Technol.*, *15*, 371–384.

Borkink, J.G.H., & Westerterp, K.R. (1992). Influence of tube and particle diameter on heat transport in packed beds. *A.I.Ch.E. J.*, *38*, 703–715.

Borman, P.C., Bos, A.N.R., & Westerterp, K.R. (1994). A novel reactor for determination of kinetics for solid catalyzed gas reactions. *A.I.Ch.E. J.*, *40*, 862–863.

Dekker, N.J.J., Hoorn, J.A.A., Stegenga, S., Kapteijn, F., & Moulijn, J.A. (1992). Kinetics of the CO oxidation by O_2 and N_2O over $Cu–Cr/Al_2O_3$. *A.I.Ch.E. J.*, *38*, 385–396.

Dixon, A.G. (1996). An improved equation for the overall heat transfer coefficient in packed beds. *Chem. Engng and Process.*, *35*, 323–331.

Gnielinski, V. (1982). Berechnung des Wärme- und Stoffaustauschs in durchströmten ruhenden Schüttungen, *Verfahrenstechnik*, *16*, 36–39.

Hall, R.E., & Smith, J.M. (1949). Design of gas–solid reactors. *Chem. Engng Prog.*, *45*, 459–470.

Hoffman, H. (1979). Fortschritte bei der Modellierung von Festbettreaktoren, *Chemie – Ingenieur Technik*, *51*, 257–265.

Mardanova, N.M., Akhverdiev, R.B., Talyschinskii, R.M., Medzhidov, A.A., Ali-zade, F.M., & Rizaev, R.G. (1996). Oxidation of carbon monoxide on $Cu–Cr–Mn/\gamma\text{-}Al_2O_3$ catalysts from various sources. *Kinet. Catal.*, *37*, 84–89.

Schouten, E.P.S. & Borman, P.C., & Westerterp, K.R. (1994). Oxidation of ethylene in a wall-cooled packed-bed reactor. *Chem. Engng Sci.*, *49*, 4725–4747.

Schouten, E.P.S., & Westerterp, K.R. (1996). Angular temperature variations in a wall-cooled packed bed reactor. *A.I.Ch.E. J.*, *42*, 2635–2644.

Schwedock, M.J., Windes, L.C., & Ray, W.H. (1989). Steady state and dynamic modeling of packed bed reactor for the partial oxidation of methanol to formaldehyde, II. Experimental results compared with model predictions. *Chem. Engng Commun.*, *78*, 45–71.

Westerterp, K.R., Kronberg, A.E., Benneker, A.H., & Dilman-V.V. (1996). Wave concept in the theory of hydrodynamical dispersion – A Maxwellian type approach. *Chem. Engng Res. Des.*, *74*, 944–952.

Wijngaarden, R.J. & Westerterp, K.R. (1989). Do the effective heat conductivity and the heat transfer coefficient at the wall inside a packed bed depend on a chemical reaction? Weakness and applicability of current models. *Chem. Engng Sci.*, *44*, 1653–1663.